

Article

Effect of Sintering Parameters on Microstructural Evolution of Low Sintered Geopolymer Based on Kaolin and Ground-Granulated Blast-Furnace Slag

Noorina Hidayu Jamil ^{1,2,*}, Mohd Mustafa Al Bakri Abdullah ^{1,3,*}, Wan Mohd Arif W. Ibrahim ^{1,3}, Razna Rahim ², Andrei Victor Sandu ^{4,5,*}, Petrica Vizureanu ^{4,6}, João Castro-Gomes ⁷ and José Manuel Gómez-Soberón ⁸

¹ Geopolymer & Green Technology, Centre of Excellence (CEGeoGTech), Universiti Malaysia Perlis (UniMAP), Kangar 01000, Malaysia

² Faculty of Mechanical Engineering & Technology, Universiti Malaysia Perlis (UniMAP), Arau 02600, Malaysia

³ Faculty of Chemical Engineering & Technology, Universiti Malaysia Perlis (UniMAP), Arau 02600, Malaysia

⁴ Faculty of Material Science and Engineering, Gheorghe Asachi Technical University of Iasi, 41 D. Mangeron St., 700050 Iasi, Romania

⁵ Romanian Inventors Forum, Str. Sf. P. Movila 3, 700089 Iasi, Romania

⁶ Technical Sciences Academy of Romania, Dacia Blvd 26, 030167 Bucharest, Romania

⁷ C-MADE Centre of Materials and Building Technologies, University of Beira Interior (UBI), 6201-001 Covilhã, Portugal

⁸ Barcelona School of Building Construction, Polytechnic University of Catalonia, Av. Doctor Marañón 44-50, 08028 Barcelona, Spain

* Correspondence: noorinahidayu@unimap.edu.my (N.H.J.); mustafa_albakri@unimap.edu.my (M.M.A.B.A.); sav@tuiasi.ro (A.V.S.)



Citation: Jamil, N.H.; Abdullah, M.M.A.B.; Ibrahim, W.M.A.W.; Rahim, R.; Sandu, A.V.; Vizureanu, P.; Castro-Gomes, J.; Gómez-Soberón, J.M. Effect of Sintering Parameters on Microstructural Evolution of Low Sintered Geopolymer Based on Kaolin and Ground-Granulated Blast-Furnace Slag. *Crystals* **2022**, *12*, 1553. <https://doi.org/10.3390/cryst12111553>

Academic Editors: Zhaohui Li and Indrajit Charit

Received: 9 September 2022

Accepted: 23 October 2022

Published: 31 October 2022

Publisher's Note: MDPI stays neutral with regard to jurisdictional claims in published maps and institutional affiliations.



Copyright: © 2022 by the authors. Licensee MDPI, Basel, Switzerland. This article is an open access article distributed under the terms and conditions of the Creative Commons Attribution (CC BY) license (<https://creativecommons.org/licenses/by/4.0/>).

Abstract: The effect of different sintering parameters on the mechanical properties of sintered kaolin-GGBS will influence the variation of mechanical properties of sintered kaolin-GGBS geopolymer. Based on previous research, the samples have major cracking and many large pores due to the sintering temperature and holding time during the sintering process. The first objective is to study the effect of different sintering parameters on the mechanical properties of sintered kaolin-GGBS geopolymer and the second objective is to correlate the strength properties of sintered kaolin-GGBS geopolymer with microstructural analysis. In a solid-to-liquid 2:1 ratio, kaolin and GGBS were combined with an alkali activator. The kaolin-GGBS geopolymer was then cured at room temperature for 24 h. The samples were then cured for 14 days at 60 °C, followed by using double-step sintering at temperatures of 500 °C and 900 °C with varying heating rates and holding durations. The compressive strength and shrinkage of the kaolin-GGBS geopolymer were evaluated, and the morphology was examined using a scanning electron microscope. In comparison to other samples, the sintered kaolin-GGBS geopolymer with a heating rate of 2 °C and a holding duration of 2 h had the optimum compressive strength value: 22.32 MPa. This is due to the contribution of MgO from GGBS that refines the pore and increases the strength. The 13.72% shrinkage with a densified microstructure was also obtained at this parameter due to effective particle rearrangement during sintering.

Keywords: ceramic; geopolymer; self-fluxing; sintering; kaolin; sintered geopolymer

1. Introduction

The physical and mechanical properties, as well as the durability, of geopolymer binders have been demonstrated. Geopolymer binders have been studied in a variety of applications, including concrete, coating materials, and masonry units [1]. Geopolymers have received a lot of attention because of their excellent mechanical and physical properties, low energy consumption, and low greenhouse gas emissions during fabrication [2]. Geopolymers have far more potential as regenerable catalysts, membranes, and hazardous chemical storage materials, as well as photoactive composites [2]. However, geopolymers

are composite substances that contain crystalline phases in the amorphous paste. The initial crystalline material in the geopolymers may come from either the source material or the aggregate. When exposed to high temperatures, this material will undergo phase changes, which can impact the geopolymer's bulk thermal properties [2]. Kaolin is a material with exceptional properties for ceramics such as technical porcelain, whiteware, and high-quality building ceramics [3]. It has an excellent structure formed and a wide range of firing temperatures and has low reactivity during geopolymerization. Kaolin is one of the naturally occurring abundant minerals from the Earth's crust [4]. The use of kaolin as a raw material in geopolymer however more can be found on the use of metakaolin to produce geopolymers [4]. Kaolin geopolymers were made by the alkali activation of kaolin with a substance resolution that is a mixture of NaOH and sodium silicate solutions [5]. In designing a kaolin-based geopolymer product for specific applications, parameters such as sodium hydroxide concentration and curing regime are important factors that need to be taken into consideration [6].

Ground-granulated blast-furnace slag (GGBS) is one of the most used by-product materials in the fabrication of geopolymer materials [6]. Besides, ground-granulated blast-furnace slag (GGBS) could be a glass granular material that is made because of the condition once liquefied furnace slag is quickly chilled and immersed in water throughout the formation of the iron industry. The ground-granulated blast furnace was referred to as a non-metallic product that includes silica, alumina, calcium oxide, and different bases developed in liquefied form at the same time with iron during a furnace [6,7]. The primary composition in GGBS is calcium oxide (CaO) has been reported to be an efficient element for the development of high compressive strength in a geopolymer. The hardening method improved with the addition of CaO to the composition [8]. The CaO from GGBS acted as a setting agent which leads to the hardening of the geopolymer at room temperature without affecting the mechanical properties of the final product [8]. Addition of GGBS with fly ash-based geopolymer was found to possess a positive impact on the strength even when added in tiny amounts. However, the advantages of using GGBS usually ascribe to a long-term resistance of weathering and strength gain and aggressive chemical action. Besides, it all depends on the replacement of ratio, particle size, and curing conditions [9,10].

The effect of different sintering parameters on the mechanical properties of sintered kaolin-GGBS influences the variation of mechanical properties of the sintered kaolin-GGBS geopolymer. However, it leads to different mechanical properties of the sintered geopolymer [8]. In this research, there were two steps of sintering parameters which were: step one which consisted of a sintering temperature of 500 °C and a heating rate of 2 °C/min. Meanwhile, step 2 consisted of a sintering temperature of 900 °C with a heating rate of 4 °C/min. The holding time will be varied to three levels which were 1 h, 2 h, and 3 h for each step. The purpose of sintering two steps sintering was to reduce major cracking [11]. Based on the previous research, high curing temperatures may lead to hardener and hinder proper geopolymerization and this shows that curing at higher temperatures distorted the reaction and led to the failure of the sintered kaolin-GGBS geopolymer. Direct sintering of geopolymer material at high temperatures showed excessive shrinkage and cracking of the geopolymer. The effect of sintering was influenced by many parameters, including the mineralogical part composition of the raw materials, used for the preparation of the ceramic mixtures and the temperature at which the ceramic structure is sintered [8].

2. Materials and Methods

Kaolin was obtained from Associated Kaolin Industries Sdn. Bhd., Malaysia. Kaolin has an average particle size of ~13.3 µm, and the geopolymer substance is made mostly from kaolin, which is a significant source of aluminosilicate. Ground-granulated blast-furnace slag (GGBS) with 90% of glass content was purchased from Ann Joo Integrated Steel Sdn. Bhd, Malaysia. GGBS was used as an additive in this kaolin geopolymer. Besides, GGBS's primary component is calcium oxide, which has been a practical component for developing high compressive strength in a geopolymer. NaOH flakes with a purity of 99%

were acquired from Formosa Plastic Corporation in Taiwan. Na_2SiO_3 was used and mixed with NaOH as an alkali activator. South Pacific Chemical Industries Sdn. Bhd., Malaysia, provided the liquid sodium silicate, which had a chemical composition of 30.1% SiO_2 , 9.4% Na_2O , and 60.5% H_2O ($\text{SiO}_2/\text{Na}_2\text{O}$ ratio of 3.20).

The chemical composition was characterized for kaolin using a benchtop X-ray fluorescence (XRF) spectrometer with the brand name PAN analytic of PW4030, energy disperse microprocessor-controlled analytical instrument, model type Minipal software. The samples were mixed with binder and ground in pastel mortar for five minutes. Then, the samples were pressed into pellets with a pressing machine, 20 tonnes load prior to analysis. The sample was loaded into the chamber of the spectrometer and operated at a maximum voltage of 30 kV. A maximum current of 1 mA was applied to produce an X-ray to excite the sample for a preset time (10 min). X-ray fluorescence (XRF) identified and quantified the elemental content of the unknown by exposing the materials to X-ray fluorescence radiation.

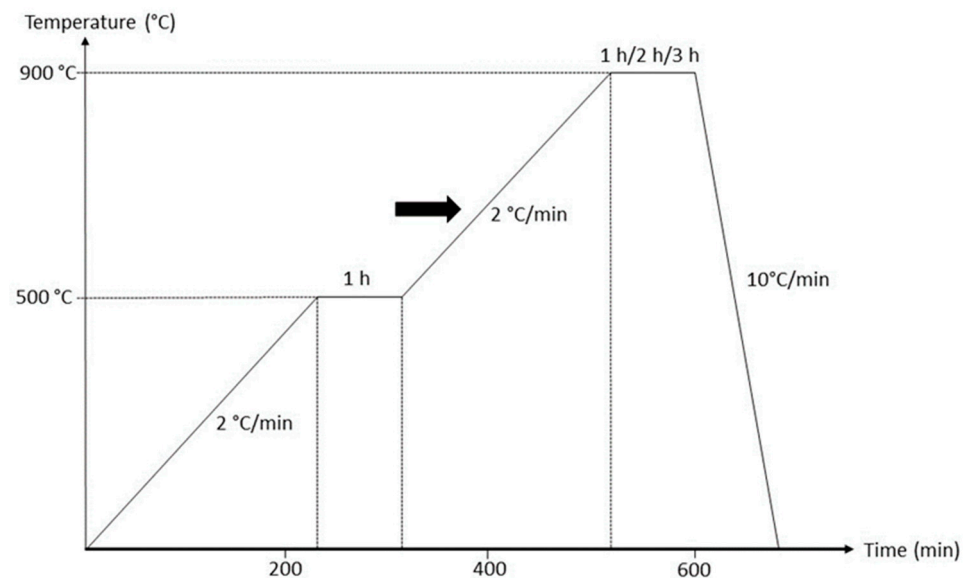
The primary chemical composition of the kaolin and GGBS was found to be silica (SiO_2) and alumina (Al_2O_3) with a total content of 85.7% for kaolin and 40.9% for GGBS as shown in Table 1. The higher mechanical strength of SiO_2 and Al_2O_3 can be achieved. While GGBS contains a huge quantity of flux in GGBS, which is composed of the total of CaO (50.37%) and MgO (3.2%), not only lowers the sintering temperature but also initiates the geopolymerization process [12]. Furthermore, kaolin contains K_2O (6.05%), which contributes to flux and decreases the melting temperature. During the ceramic sintering process, this chemical composition will serve as a self-fluxing component. Both kaolin and GGBS include a high quantity of silica (SiO_2), which melts during sintering to generate a glassy phase that links it to the ceramic body.

Table 1. Chemical composition of kaolin and GGBS.

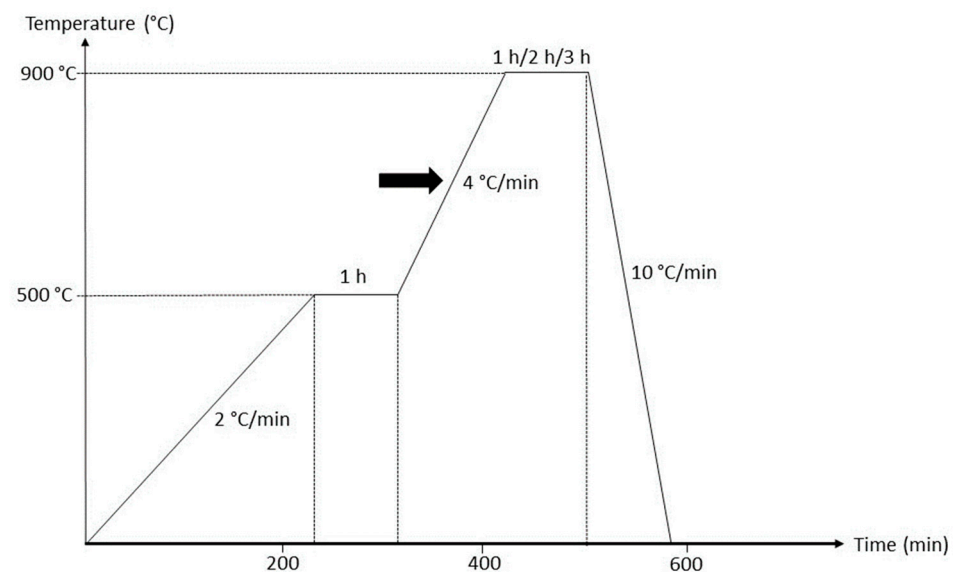
Chemical Composition (%)	Kaolin	GGBS
CaO	N/A	50.37
SiO_2	54.0	30.4
Al_2O_3	31.7	10.5
Fe_2O_3	4.89	0.53
MgO	N/A	3.2
TiO_2	1.41	0.98
K_2O	6.05	N/A
ZrO_2	0.10	0.05
MnO_2	0.11	0.71
LOI	1.74	0.32

Alkali activator was first prepared by mixing the sodium hydroxide (NaOH) and sodium silicate (Na_2SiO_3) with a solid-to-liquid ratio of 4:1 by using a mechanical stirrer for 15 min. The alkali activator was prepared 24 h prior to use by mixing 8 M NaOH solution. Then, kaolin and GGBS were mixed together with an alkali activator by using a ratio of 2:1. After that, kaolin-GGBS geopolymer was poured into a $50 \times 50 \times 50$ mm mold size. The geopolymer slurry was vibrated to remove the trapped air, and sealed with plastic at the exposed portion of the mold during the curing stage. The samples were allowed to cure at room temperature for 24 h. After 24 h of curing at room temperature, all samples were then cured for 14 days at 60 °C in the oven. After being cured for 14 days at 60 °C, 3 sets of samples were sintered in LT Muffle Furnace. The sintering process was carried out in two steps of the sintering process: the first step with a temperature of 500 °C and the second step at 900 °C with different heating rates and holding times and 10 °C/min of cooling rates elucidated in Figure 1a,b. The samples were then examined for shrinkage,

compressive strength, microstructure analysis, and phase analysis. The sintered samples were labeled according to the parameter of sintering namely as shown in Table 2 below.



(a)



(b)

Figure 1. Sintering profile with different heating rate for step 2 (a) 2 °C/min and (b) 4 °C/min.

Table 2. Labeling for sintered samples.

Holding Time (h)/Heating Rate (°C/min)	2 °C/min	4 °C/min
1 h	A1	B1
2 h	A2	B2
3 h	A3	B3

Shrinkage is strain associated with the loss of moisture from the kaolin-GGBS geopolymer by evaporation of water or hydration of ceramic. To conduct the test, the size of the specimens was 50 × 50 × 50 mm was taken the length before sintering and after sintering. The specimens were first cured at room temperature for 24 h, then dried in an oven

for 14 days at a temperature of 60 °C followed by sintering at 900 °C. The dimensional shrinkage was determined using Equation (1) [13]. L1 is the initial length and L2 is after the sintering length. The measurement was taken before curing in the oven at 60 °C and after sintering at a temperature of 900 °C.

$$SL = (L1 - L2)/L2 \times 100\% \quad (1)$$

The compressive strength testing was carried out following ASTM C109 by using a Shimadzu Universal Testing machine device, equipped with compressive units. Three samples were tested to get an average value on compressive strength. Samples were kept sealed in a shrink-wrap bag before it was tested. Loading displacement was controlled at a constant rate of 0.5 mm/min. Tests were carried out with normalized cubical samples having a dimension of (50 × 50 × 50) mm. Sample surfaces were previously polished to ensure the best surface quality (parallelism, planarity). All values of the maximum compressive strength reported in this study are mean values over three tests under the same conditions. The strength was recorded in N/mm² based on Equation (2).

$$\sigma = F/A \quad (2)$$

where σ is compressive strength, F is the applied load in Newton (N) unit, and A is a cross-sectional area in mm².

The microstructural was characterized for kaolin, GGBS, and all sintered geopolymers by scanning electron microscopy (SEM) using TESCAN VEGA 4th with a secondary electron detector. The accelerating voltage used was 10–15 kV and secondary electron EDS detector. Since the raw kaolin and GGBS were in powder form, therefore for the sample preparation, the powder was sprinkled onto a double-sided carbon tape and blown to remove the loosely held powder. For sintered kaolin-GGBS geopolymer, the internal surface cross-sectioned of the solid sample was characterized. The section pieces were taken prior to the compressive test. The specimen was then coated with Au-Pd as a conductive medium to improve image quality and resolution.

The phase composition of the kaolin, GGBS, as-cured, and sintered kaolin-GGBS geopolymer was determined using the X-ray diffraction method (XRD) (BRUKER D8 ADVANCE), equipped with a copper anode (Cu K α , λ 1.5406 Å) 40 kV and 20 mA. Prior to analysis, dry powder was compacted and analysis was recorded within 2 θ from 5 θ to 80 θ using a step size of 0.05 θ and counting time of 5 s per step with a scan rate of 0.1 s/sec. The data were analyzed using the X'Pert HighScore Plus software. The XRD patterns were recorded in the range silicon powder was used as a standard agent to remove the instrumental broadening effects from the observed profile broadening.

3. Results

3.1. Physical Observation of Low Sintered Kaolin-GGBS Geopolymer

Figure 2 shows the physical observation of sintered kaolin-GGBS geopolymer samples with different heating rates and holding times. As can be seen on the surface of samples A, it has no major cracking when sintered at 2 °C/min with 2 h of holding time while B has significant cracking due to internal stresses when the drying shrinkage is too severe after sintered at 4 °C/min with 3 h of holding time. Another problem with drying is the amount of energy necessary to evaporate water. Furthermore, due to the use of a heating rate of 4 °C/min during the second step of sintering with 3 h of holding time, sample B had surface cracking. This demonstrates that a longer holding time and a faster heating rate applied pressure to the sample, causing substantial cracking.

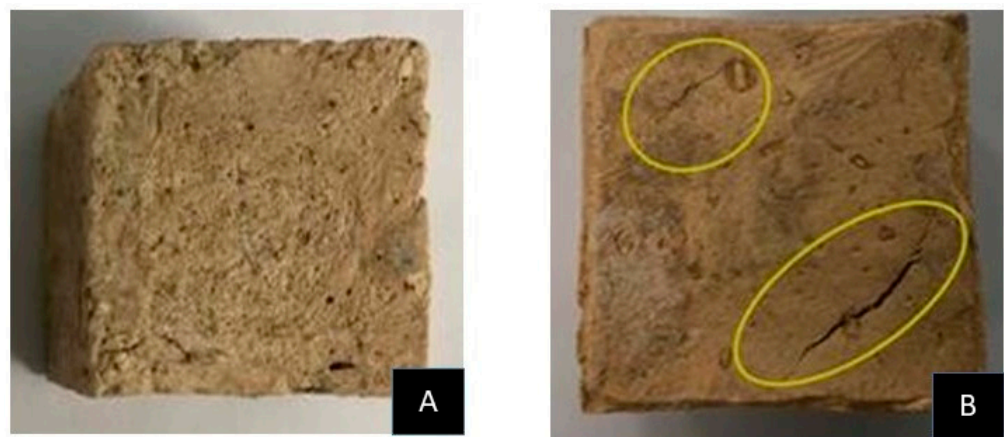


Figure 2. Physical observation of sintered kaolin-GGBS geopolymer.

Figure 3 demonstrates the shrinkage observation on each sample with different heating rates and holding times. Sample A2 has the highest percentage of shrinkage, which is 14.44%, by the heating rate of 2 °C/min at the first and second step of the temperature with a holding time of 1 h. While, sample B2 with 13.72% of shrinkage which means denser, less water absorption. The lowest percentage of shrinkage was sample D4 with 9.9% by the different heating rates at the first step, which is 2 °C/min, and the second step is 4 °C/min with 1 h of holding time due to high pressure. Thus, the effects of heating rate and holding time have impacted the samples. However, these two samples show that heating rate and holding time dramatically affect the sample's physical dimensions. The geopolymer experiences various modifications during sintering, such as the removal of water and the creation of a newborn crystalline phase. Due to the cohering together of incoherent particles during the sintering process, the surface energy lowers. As a result, the overall surface area is reduced. The samples melted when the sintering temperature was increased to 1250 °C, which was above the kaolin geopolymer's melting point [14].

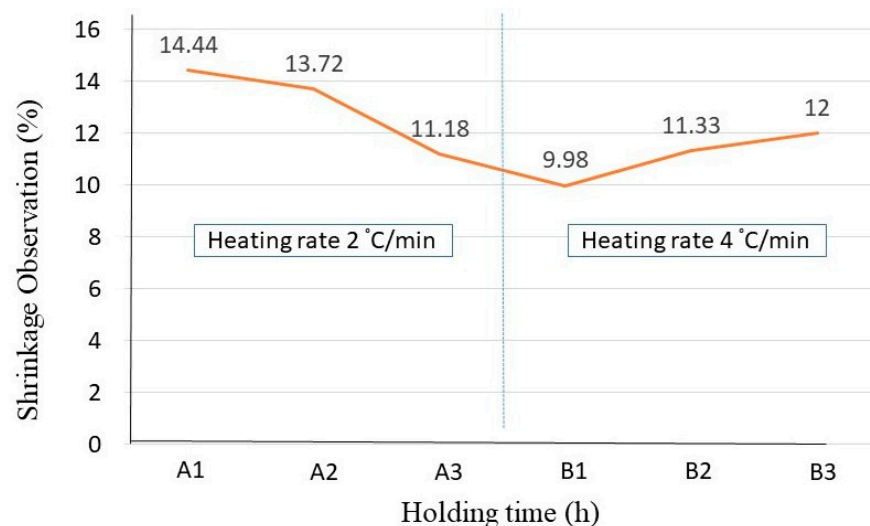


Figure 3. Shrinkage observation on different holding times (1:1 h, 2:2 h, and 3:3 h) and heating rates.

3.2. Microstructural Evolution of Low Sintered Kaolin-GGBS Geopolymer

The highest compressive strength which is 22.32 MPa was obtained at a heating rate of 2 °C/min for 2 h of holding time at 900 °C temperature, as shown in Figure 4, as a result of reactive MgO to the GGBS create geopolymer paste, which refines the pore size and increases compressive strength [15]. The CaO composition from GGBS works as a setting agent, causing the finished product to harden at room temperature without

compromising its mechanical qualities. Furthermore, the mixed alkali activator's content has a substantial impact on compressive strength. The lowest compressive strength was 4.36 MPa with a heating rate of 4 °C/min of 3 h holding time owing to excessively high pressure from the holding time and heating rate which led to major cracking. This indicates that a higher heating rate has a significant impact on the microstructure. The crystalline phase, which influences the strength of glass-ceramic, is the second determining component. A high-volume proportion of crystallinity is required to achieve high compressive strength. Furthermore, the curing temperature has a considerable impact on the mechanical properties of the kaolin-GGBS geopolymer. Furthermore, a longer curing time aided the geopolymerization process and resulted in greater strength growth. The reaction mechanism of GGBS characteristics has a significant impact on strength and durability. Hence, the strength of the geopolymer degrades as a result of the activator silicate solution, which is a delayed response. The mixture of sodium silicate and sodium hydroxide solution ratio also has a significant impact on the hardened geopolymer strength [16].

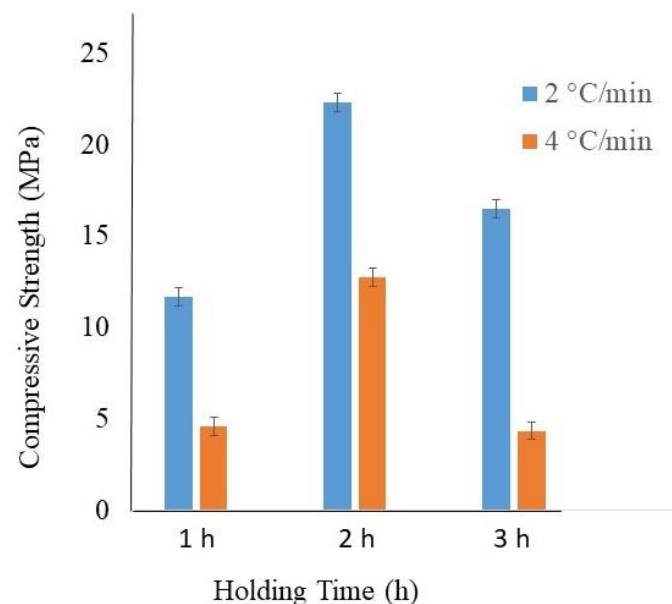


Figure 4. Compressive strength at different holding time (1 h, 2 h, and 3 h).

Based on Figure 5, the microstructure of sintered geopolymer when opposed to 2 °C/min resulted in fewer pores and more densified, while the microstructure at 4 °C/min reveals an increased number of pores and untreated kaolin. Sintered geopolymer with 2 °C/min of heating rate and 2 h of holding time is more densified with small pores and the highest compression strength obtained, 22.32 MPa. This is due to the slow heating rate and longer holding time. On the contrary, sintered geopolymer with 4 °C/min and 3 h of holding time resulted in the lowest compressive strength and major cracking. The microstructure of untreated kaolin was observed at 2 °C/min and 3 h indicating that longer holding time for geopolymer did not allow such improvement of the packing density and homogenization of the microstructure during phase transformation [17]. This phenomenon induced the appearance of large pores and therefore led to lower sinterability. During the holding process, the surface energy of the individual particles contacted with one another thus forming a necking and forming a grain hence reducing the empty spaces of pores. The continuous growth of grains initiates grain boundaries, consequently densifying and eliminating the pores. The increase in holding time is due to the convergence of particles, which allows full coalescence of the particles and induces viscous flow which is necessary for densification [18,19]. For the low rate-heated sample, the longer heating step in temperature resulted in more effective particle rearrangement during phase transition from transition to alumina.

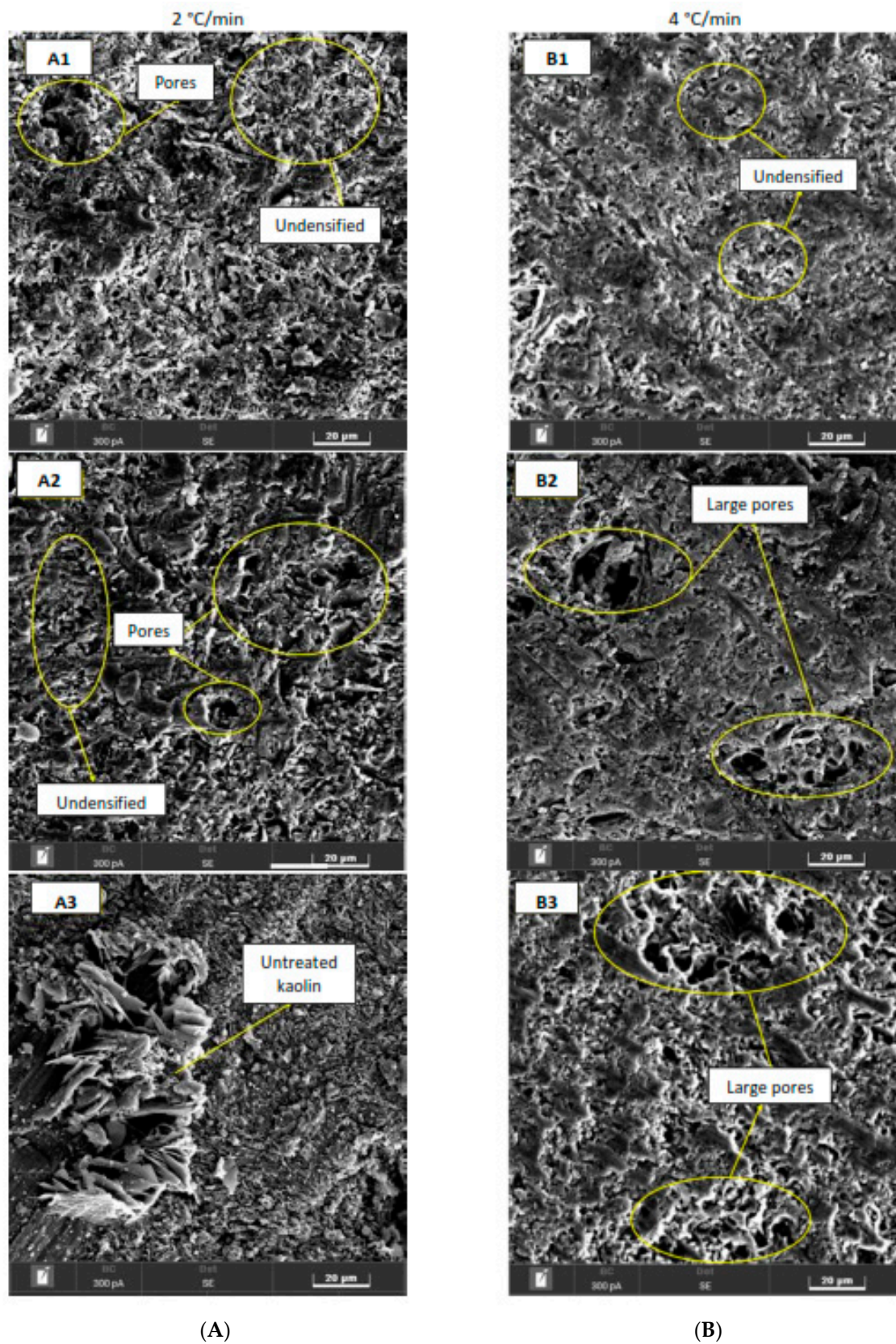


Figure 5. Microstructure of sintered kaolin-GGBS geopolymer with different heating rates (2 °C/min and 4 °C/min) and holding times (1 h, 2 h, and 3 h). (A) heating rate of 2 °C/min and (B) Heating rate of 4 °C/min.

The formation of pores indicates an aggregation, forming a larger irregular and elongated formation with thin walls, as can be seen in the image. The formation of interconnected pores confirms the evaporation of water from the structure during sintering. The movement of water evaporation during sintering is illustrated in Figure 6.

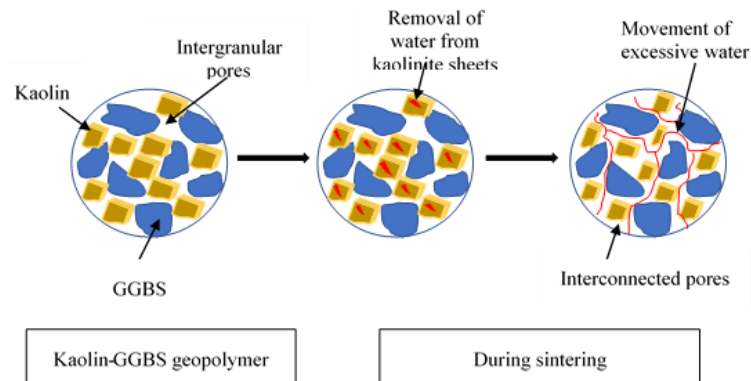


Figure 6. Illustration on the movement of water evaporation during sintering.

Figure 7 shows the phase transformation of kaolin-GGBS geopolymer before and after sintering at 2 °C/min of heating rate and 2 h of holding time. The main phase obtained before sintering was kaolinite. Kaolinite ($\text{Al}_4(\text{OH})_8(\text{Si}_4\text{O}_{10})$) was not visible after sintering. However, nepheline (Si-rich) $\text{Na}_7(\text{Al}_6\text{Si}_{10}\text{O}_{32})$ occurred after sintering. The presence of nepheline in sintered samples leads to an increase in the compressive strength. The formation of albite and nepheline after sintering was influenced by a reaction between kaolinite and alkali activator. Sodium silicate (Na_2SiO_3) can provide sufficient silicon ions during the hardening process to promote the activation precursor of geopolymer materials and improve the mechanical properties [20]. The growth from the nuclei will fix the formation of the geopolymer backbone and form the solid framework [21,22]. Albite and nepheline consist of the same elements which are Na, Al, Si, and O. During geopolymerization, the function of Na cations was to balance the negative charges created by the formation of Si-O-Al bonding, or nonbridging oxygen ions remained in the system. Meanwhile, OH⁻ is consumed during the hydrolysis of kaolin. The Na_2O content was contributed by the Na_2SiO_3 solution and NaOH solution. Therefore, most of the gained strength arises from the GGBS in addition to the enhancement effect of the NaO from the alkali activator. The densified area in sintered kaolin-GGBS geopolymer was contributed from Na_2O .

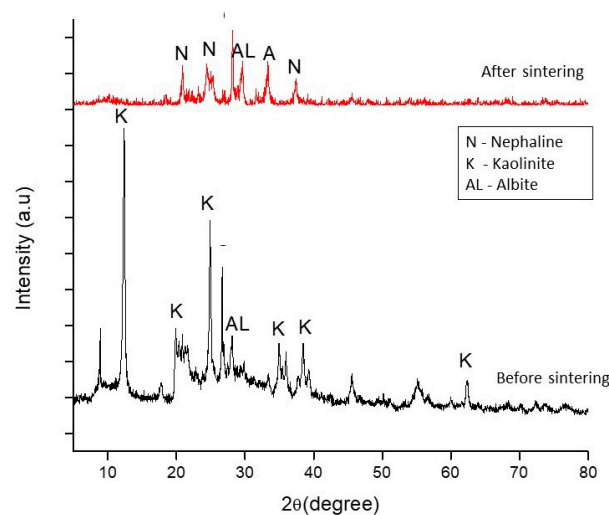


Figure 7. Phase analysis of kaolin-GGBS geopolymer before and after sintering.

4. Conclusions

In conclusion, the effect of different sintering parameters on the mechanical properties of sintered kaolin-GGBS geopolymer shows optimum strength and densification at a heating rate of 2 °C/min and 2 h of holding time. The highest compression strength obtained was 22.32 MPa. Meanwhile, the lowest is at 4 °C/min and 3 h of holding time with 4.36 MPa of compressive strength. Densification was increased during the sintering process, resulting in a decrease in porosity and greater mechanical strength. This shows that heating rate and holding time influenced the sintering geopolymer ceramic. A higher heating rate did not influence the packing density and microstructure homogenization, therefore resulting in the appearance of large pores and consequently lower sinterability. Two hours of holding time resulted in optimum microstructural properties of low-sintered geopolymer based on kaolin and ground-granulated blast-furnace slag.

Author Contributions: Conceptualization, N.H.J. and M.M.A.B.A.; methodology, N.H.J., M.M.A.B.A. and R.R.; software, N.H.J. and W.M.A.W.I.; validation A.V.S. and M.M.A.B.A.; formal analysis, N.H.J. and R.R.; investigation, N.H.J., M.M.A.B.A. and P.V.; resources, N.H.J. and R.R. data curation, N.H.J. and J.C.-G.; writing—original draft preparation N.H.J. and W.M.A.W.I.; writing—review and editing, M.M.A.B.A. and A.V.S.; visualization, N.H.J. and R.R.; supervision, M.M.A.B.A. and A.V.S.; project administration, N.H.J.; funding acquisition, M.M.A.B.A. and J.M.G.-S. All authors have read and agreed to the published version of the manuscript.

Funding: This research was funded by Ministry of Higher Education, Malaysia, through the Fundamental Research Grant Scheme (FRGS) under reference number FRGS/1/2020/TK0/UNIMAP/01/2. This publication was supported by TUIASI from the University Scientific Research Fund (FCSU).

Data Availability Statement: Not applicable.

Acknowledgments: The authors gratefully acknowledge the Ministry of Higher Education, Malaysia, through the Fundamental Research Grant Scheme (FRGS) under reference number FRGS/1/2020/TK0/UNIMAP/01/2. The authors would like to acknowledge Geopolymer and Green Technology, Centre of Excellence (CEGeoGTech), University Malaysia Perlis (UniMAP), Faculty of Mechanical Engineering and Technology and Faculty of Chemical Engineering and Technology UniMAP for the support.

Conflicts of Interest: The authors declare no conflict of interest.

References

1. Ahmari, S.; Zhang, L. The properties and durability of alkali-activated masonry units. In *Handbook of Alkali-Activated Cements, Mortars and Concretes*; Elsevier Inc.: Amsterdam, The Netherlands, 2015; pp. 643–660.
2. Brus, J.; Abbrent, S.; Kobera, L.; Urbanova, M.; Cuba, P. Advances in ²⁷Al MAS NMR Studies of Geopolymers. In *Annual Reports on NMR Spectroscopy*; Academic Press Inc.: Cambridge, MA, USA, 2016; Volume 88, pp. 79–147.
3. Štubňa, I.; Šín, P.; Trník, A.; Veinthal, R. Mechanical properties of kaolin during heating. *Key Eng. Mater.* **2012**, *527*, 14–19. [[CrossRef](#)]
4. Zhang, Z.; Zhu, H.; Zhou, C.; Wang, H. Geopolymer from kaolin in China: An overview. *Appl. Clay Sci.* **2016**, *119*, 31–41. [[CrossRef](#)]
5. Heah, C.Y.; Kamarudin, H.; Al Bakri, A.M.M.; Bnhussain, M.; Luqman, M.; Nizar, I.K.; Ruzaidi, C.M.; Liew, Y.M. Kaolin-based geopolymers with various NaOH concentrations. *Int. J. Miner. Met. Mater.* **2013**, *20*, 313–322. [[CrossRef](#)]
6. Jamil, N.H.; Abdullah, M.M.A.B.; Pa, F.C.; Mohamad, H.; Ibrahim, W.M.A.W.; Chairprapa, J. Influences of SiO₂, Al₂O₃, CaO and MgO in phase transformation of sintered kaolin-ground granulated blast furnace slag geopolymer. *J. Mater. Res. Technol.* **2020**, *9*, 14922–14932. [[CrossRef](#)]
7. Aziz, I.H.; Abdullah, M.M.A.B.; Salleh, M.M.; Azimi, E.A.; Chairprapa, J.; Sandu, A.V. Strength development of solely ground granulated blast furnace slag geopolymers. *Constr. Build. Mater.* **2020**, *250*, 118720. [[CrossRef](#)]
8. Jamil, N.; Abdullah, M.; Pa, F.C.; Hasmaliza, M.; Ibrahim, W.W.; Aziz, I.A.; Jež, B.; Nabialek, M. Phase transformation of Kaolin-ground granulated blast furnace slag from geopolymerization to sintering process. *Magnetochemistry* **2021**, *7*, 32. [[CrossRef](#)]
9. Zannerni, G.M.; Fattah, K.P.; Al-Tamimi, A.K. Ambient-cured geopolymer concrete with single alkali activator. *Sustain. Mater. Technol.* **2019**, *23*, e00131. [[CrossRef](#)]
10. Higashiyama, H.; Sappakittipakorn, M.; Mizukoshi, M.; Takahashi, O. Efficiency of ground granulated blast-furnace slag replacement in ceramic waste aggregate mortar. *Cem. Concr. Compos.* **2014**, *49*, 43–49. [[CrossRef](#)]
11. Lóh, N.J.; Simão, L.; Faller, C.; De Noni, A.; Montedo, O.R.K. A review of two-step sintering for ceramics. *Ceram. Int.* **2016**, *42*, 12556–12572. [[CrossRef](#)]

12. Rincón, A.; Desideri, D.; Bernardo, E. Functional glass-ceramic foams from ‘inorganic gel casting’ and sintering of glass/slag mixtures. *J. Clean. Prod.* **2018**, *187*, 250–256. [[CrossRef](#)]
13. Hasanah, N.; Shukor, A.; Samadi, M.; Shafegat, A.; Ariffin, N.F. Effect of Homogenous Ceramic Waste on Drying Shrinkage of Mortar. *J. Environ. Treat. Tech.* **2016**, *4*, 149–152.
14. Jaya, N.A.; Abdullah, M.M.A.B.; Ghazali, C.M.R.; Binhussain, M.; Hussin, K.; Ahmad, R. Characterization and microstructure of kaolin-based ceramic using geopolymerization. *Key Eng. Mater.* **2016**, *700*, 3–11. [[CrossRef](#)]
15. Wang, H.; Li, C.; Peng, Z.; Zhang, S. Characterization and thermal behavior of kaolin. *J. Therm. Anal.* **2011**, *105*, 157–160. [[CrossRef](#)]
16. Reddy, K.N.; Narayana, K.S.; Reddy, J.D.; Chandra, B.S.; Kumar, Y.H. Effect of sodium hydroxide and sodium silicate solution on compressive strength of metakaolin and GGBS geopolymer. *Int. J. Civ. Eng. Technol.* **2017**, *8*, 1905–1917.
17. Ahmad, R.; Ibrahim, W.M.W.; Abdullah, M.M.A.B.; Pakawanit, P.; Vizureanu, P.; Abdullah, A.S.; Sandu, A.V.; Zaidi, F.H.A. Geopolymer-Based Nepheline Ceramics: Effect of Sintering Profile on Morphological Characteristics and Flexural Strength. *Crystals* **2022**, *12*, 1313. [[CrossRef](#)]
18. Palmero, P.; Lombardi, M.; Montanaro, L.; Azar, M.; Chevalier, J.; Garnier, V.; Fantozzi, G. Effect of heating rate on phase and microstructural evolution during pressureless sintering of a nanostructured transition alumina. *Int. J. Appl. Ceram. Technol.* **2009**, *6*, 420–430. [[CrossRef](#)]
19. Aliyah, L.H.; Izzat, B.M.; Hasmaliza, M.; Katrina, A.T. Effect of mechanical properties on sintered lithium aluminosilicate glass ceramic and its thermal shock resistance properties. *AIP Conf. Proc.* **2020**, *2267*, 020047.
20. Lo, K.-W.; Lin, W.-T.; Lin, Y.-W.; Cheng, T.-W.; Lin, K.-L. Synthesis Metakaolin-Based Geopolymer Incorporated with SiC Sludge Using Design of Experiment Method. *Polymers* **2022**, *14*, 3395. [[CrossRef](#)]
21. Zhu, X.; Qian, H.; Wu, H.; Zhou, Q.; Feng, H.; Zeng, Q.; Tian, Y.; Ruan, S.; Zhang, Y.; Chen, S.; et al. Early-Stage Geopolymerization Process of Metakaolin-Based Geopolymer. *Materials* **2022**, *15*, 6125. [[CrossRef](#)] [[PubMed](#)]
22. Ma, S.; Zhang, Z.; Liu, X. Comprehensive Understanding of Aluminosilicate Phosphate Geopolymers: A Critical Review. *Materials* **2022**, *15*, 5961. [[CrossRef](#)] [[PubMed](#)]